

Resistive MHD modeling of Coaxial Helicity Injection (CHI) in NSTX

Bick Hooper, LLNL
Roger Raman, PPPL
Jon Menard, PPPL
Carl Sovinec, U. Wisconsin

Division of Plasma Physics
American Physical Society
Chicago, IL, November 8-12, 2010

This work was performed under the auspices of the U.S. Department of Energy by Lawrence Livermore National Laboratory under Contract DE-AC52-07NA27344, by Princeton Plasma Physics Laboratory under Contract DE-FG02-99ER54519, and by the PSI Center (University of Wisconsin) under Grant DE-FC02-05ER54813



ABSTRACT: CHI has been demonstrated to generate a plasma with current, density, and temperature appropriate for startup in NSTX¹ offering the potential of solenoid-free operation of an advanced ST. Whole-device simulations using the NIMROD MHD code² have been initiated to extend the understanding of the physics of CHI in NSTX and other STs and to help guide experiments and extensions. A computational grid has been developed and boundary conditions applied for external magnetic fields including eddy currents in walls and stabilizing plates. The injection and absorber slots are modeled with current specified at the injector and ExB drift at the absorber to prevent compression of the vacuum toroidal magnetic field, as done in previous simulations on HIT-II.³ Initial results will be presented and compared with experiment. The results will also be compared with simulations of the SSPX spheromak⁴ to help understand the different behaviors in the ($q>1$) ST and ($q<1$) spheromak.

¹R. Raman, et al., PRL 104, 095003 (2010).

²C.R. Sovinec, et al., J. Comp. Phys. 195, 355 (2004).

³R.A. Bayless, C.R. Sovinec and A.J Redd, unpublished.

⁴E. B. Hooper, et al., PoP 15, 032502 (2008).



Overview

- **NSTX experiments** — demonstrate that CHI is an effective, non-inductive method of generating a startup plasma
- **Our goal** — develop a whole-device, MHD simulation to:
 - **Interpret experimental results**
 - **Guide future experiments**
- **Injection model** — based on simulations of CHI in HIT-II

Initial results — **simplified physics** — **axisymmetric, no thermal conductivity**

Reported here — **tests to validate the approach and examine the sensitivity to grid and numerical parameters**

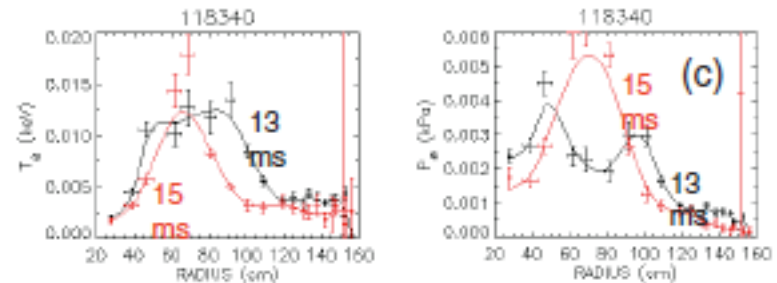
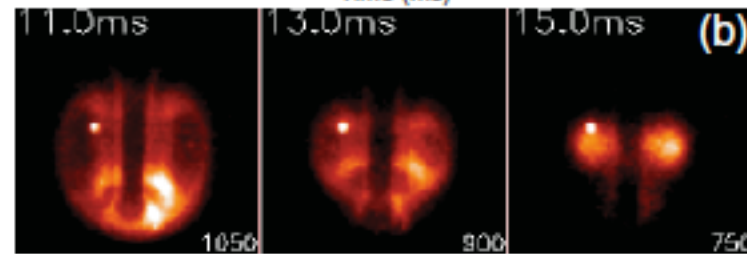
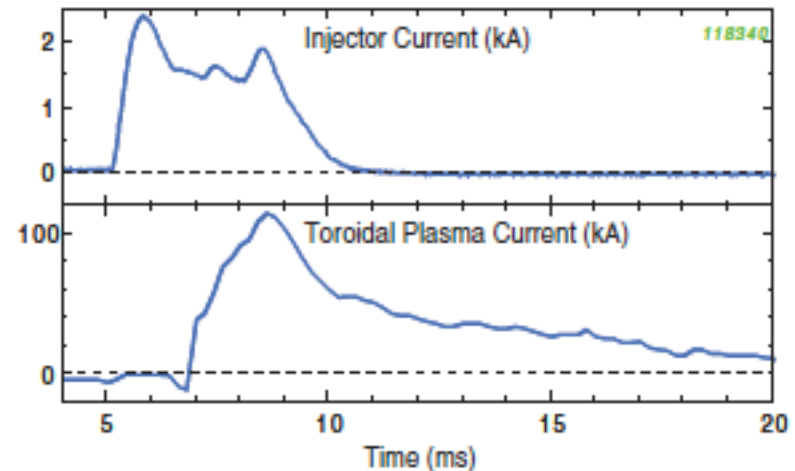
Flux expansion and plasma current agree qualitatively with experiment although detailed comparisons have not been made



NSTX reference shot

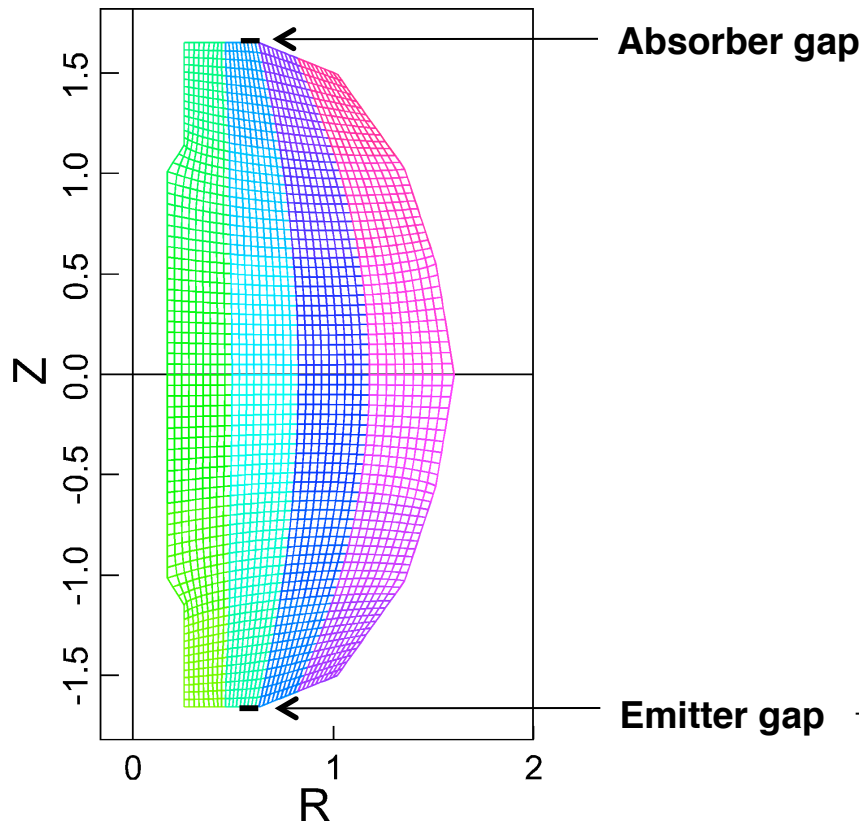
Initial simulations use parameters characteristic of NSTX Shot 118340.

[See R. Raman, et al. Phys. Rev. Letters 97, 175002 (2006)]

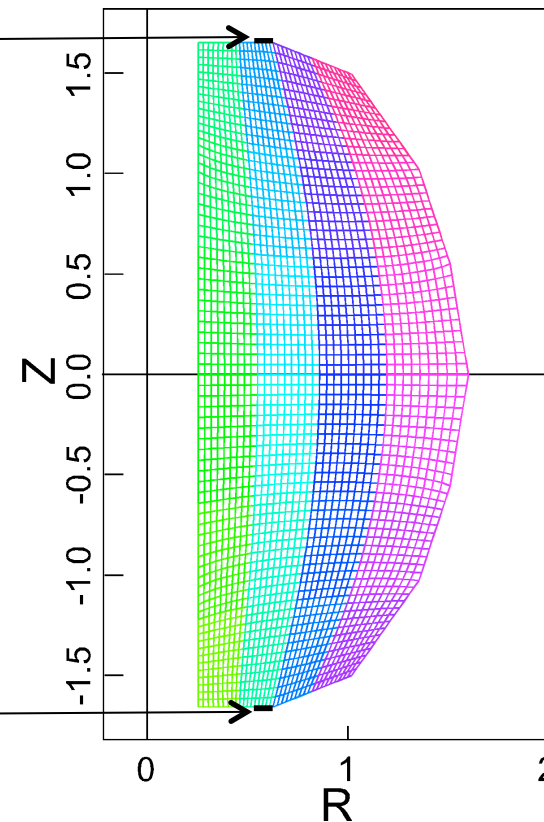


Grids for Nimrod simulations

Experimental central column



Straight central column



Grid size: 36x72. Results with grid size 60x120 agree well with 36x72

Emitter and absorber slot widths are variable. Experimental width $\approx 0.07\text{m}$

Most simulations use a width $\approx 0.11\text{ m}$ for good numerical resolution

Vacuum poloidal magnetic field

Two options are available for applying the vacuum poloidal magnetic field

- (1) External magnetic coils with currents from the experimental run
 - Presently, the code does not use time-varying fields generated using the coils
 - For these tests, the fields at $t=0$ were used
- (2) Time-varying vacuum fields on the boundary calculated using the PPPL “LRDFIT” code developed by Jon Menard
 - This option includes eddy currents in the NSTX structure and conducting (passive) plates

The results presented here use option (1)



Helicity injection model

The HIT-II model has been extended to NSTX

Emitter gap: rB_φ in the gap — increased relative to the vacuum value, representing the injected current ($rB_\varphi = \mu_0 I_{inj}/2\pi$)

Absorber gap: An electric field, $E = E_v(r_{abs,min}/r)$, is applied across the gap, generating an ExB flow out of the machine, with

$$E \times B = E_v \left(r_{abs,min} / r \right) B_\varphi \left(rB_\varphi / \left(rB_\varphi \right)_{vac} \right)$$

- Inflow at the emitter — scaled to avoid significant expansion or compression of toroidal flux as the ExB drift removes vacuum toroidal flux from the emitter

At present — the electric field and current are chosen separately and not constrained by plasma and power-supply responses

Physics approximations for initial simulations

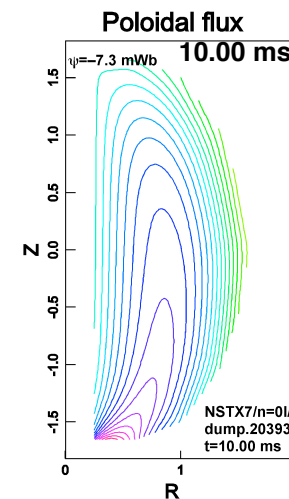
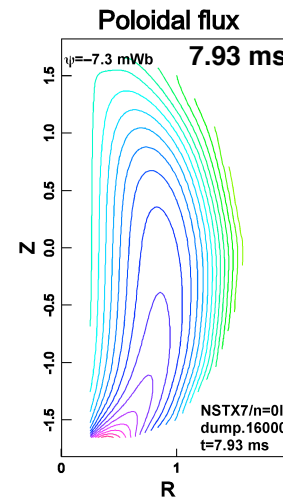
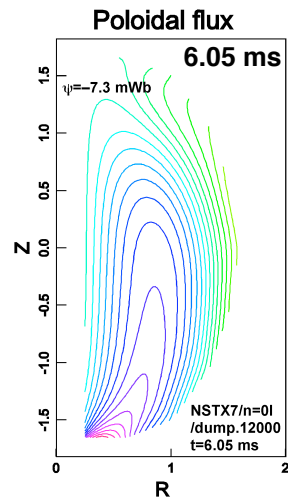
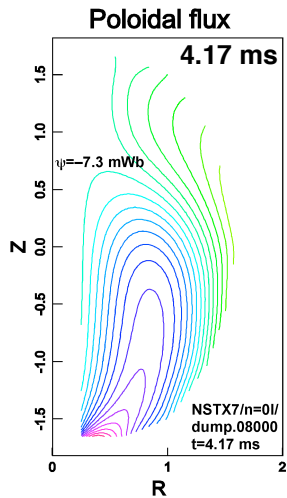
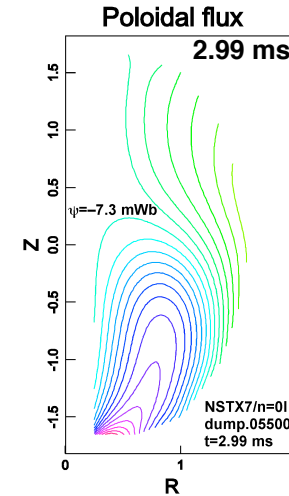
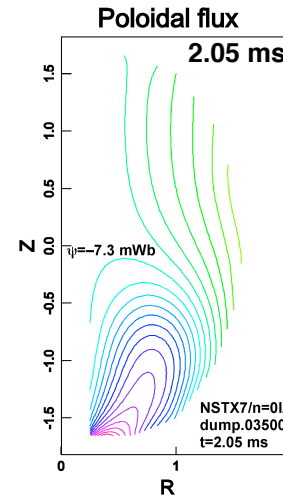
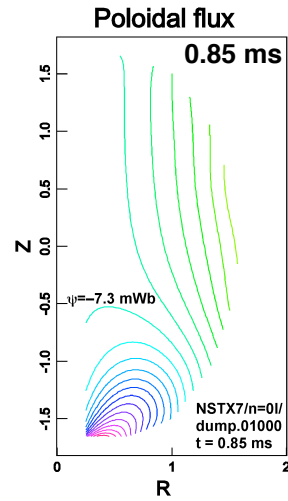
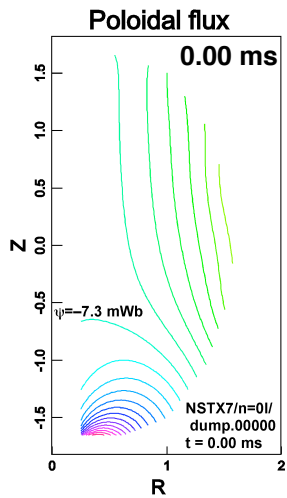
- **Axisymmetry (n=0 mode only)**
- **Constant temperature ≈ 10 eV**
Electrical diffusivity (η/μ_0) = 13 m²/s
- **A layer with high resistivity and viscosity along the top and bottom boundaries allows the injected current to diffuse along these surfaces. The electrical diffusivity (η/μ_0) is multiplied by the factor**

$$\left(1 + \left(\sqrt{dvac} - 1 \right) \left| y / y_{max} \right|^{dexp} \right)^2$$

For most calculations, $dvac = 30$, $dexp = 20$; $y_{min} = -y_{max}$

- **Kinematic viscosity = 1 – 500 m²/s**
(Most calculations used 500 m²/s)

Poloidal flux expansion – contour plots – during injection: Straight central column



Poloidal flux expansion during injection

— position of the flux-bubble top

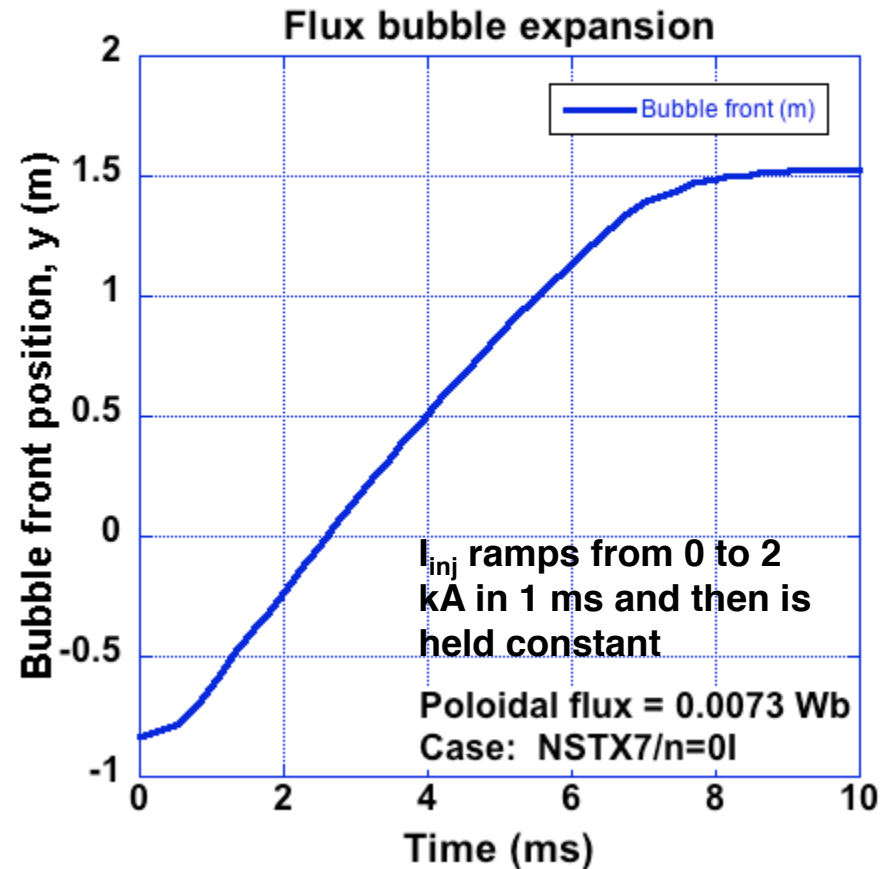
Time evolution:

Applied (injection) electric field and current

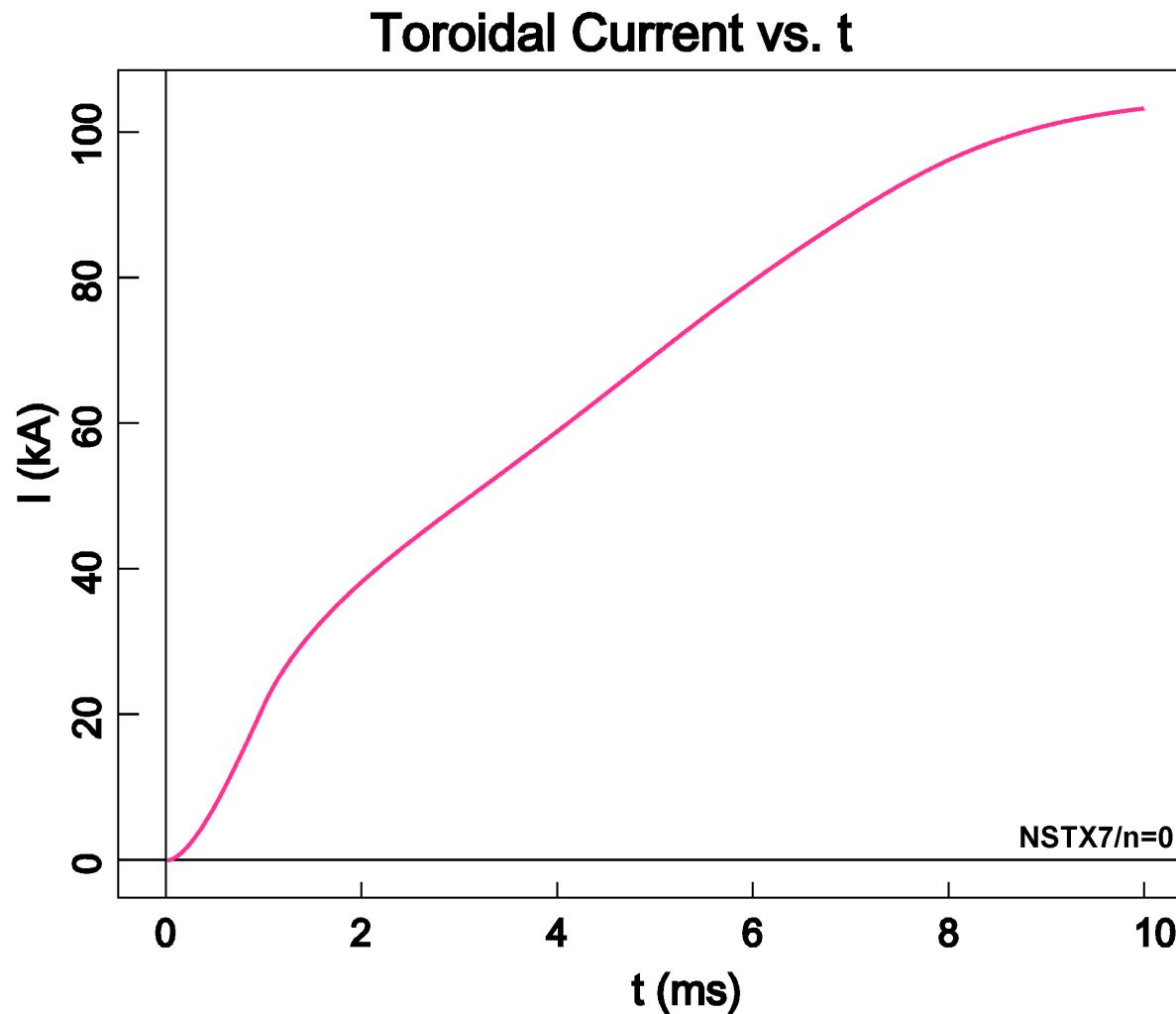
- ramped from 0 to their maxima in 1 ms, and then held constant

In this simulation:

$$E_v = 4 \text{ kV/m}$$
$$rB_\varphi = 4 \times 10^{-4} \text{ m-T}$$
$$(I = 2 \text{ kA})$$



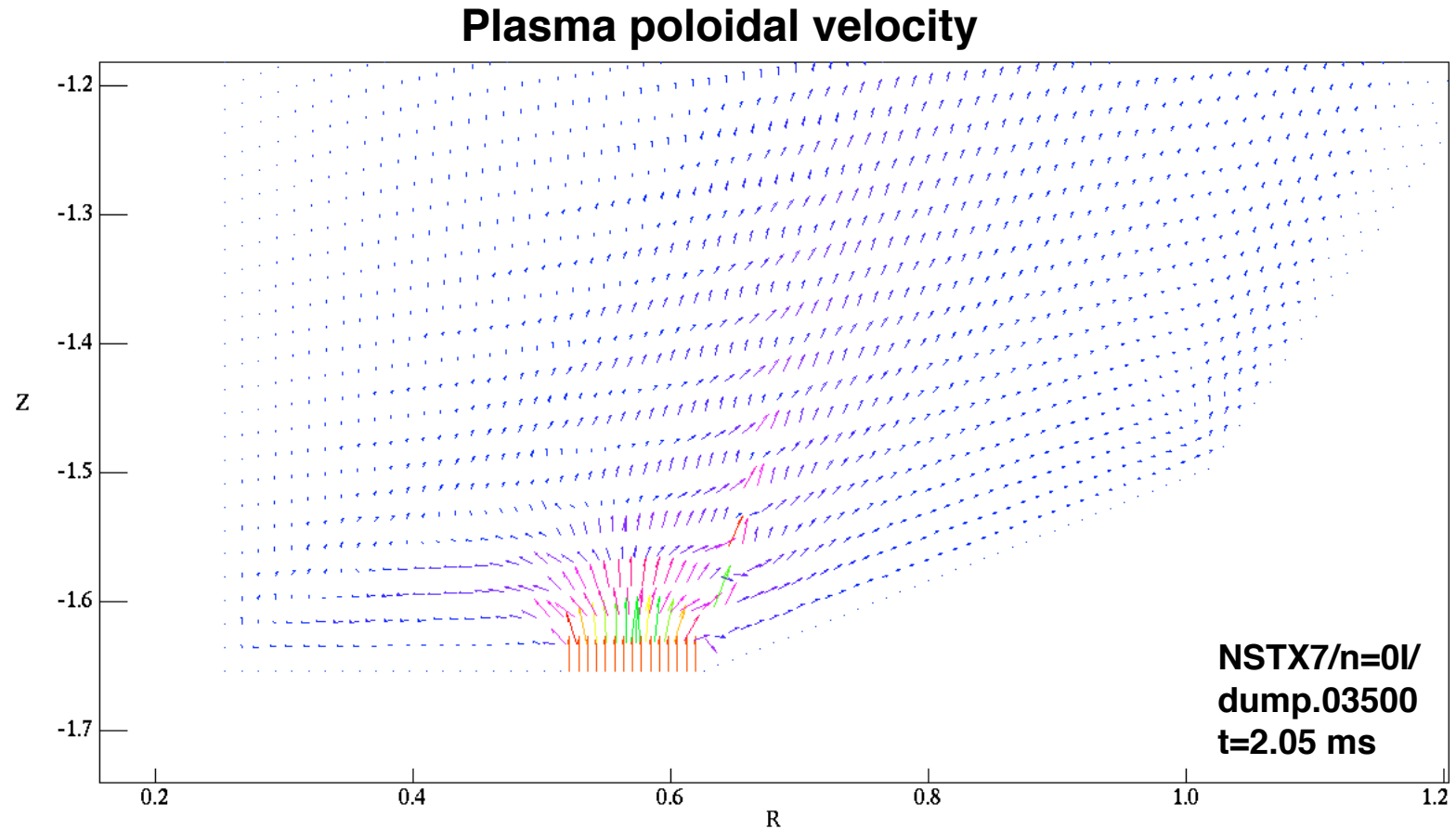
The toroidal current builds up to 100 kA, in good agreement with experiment



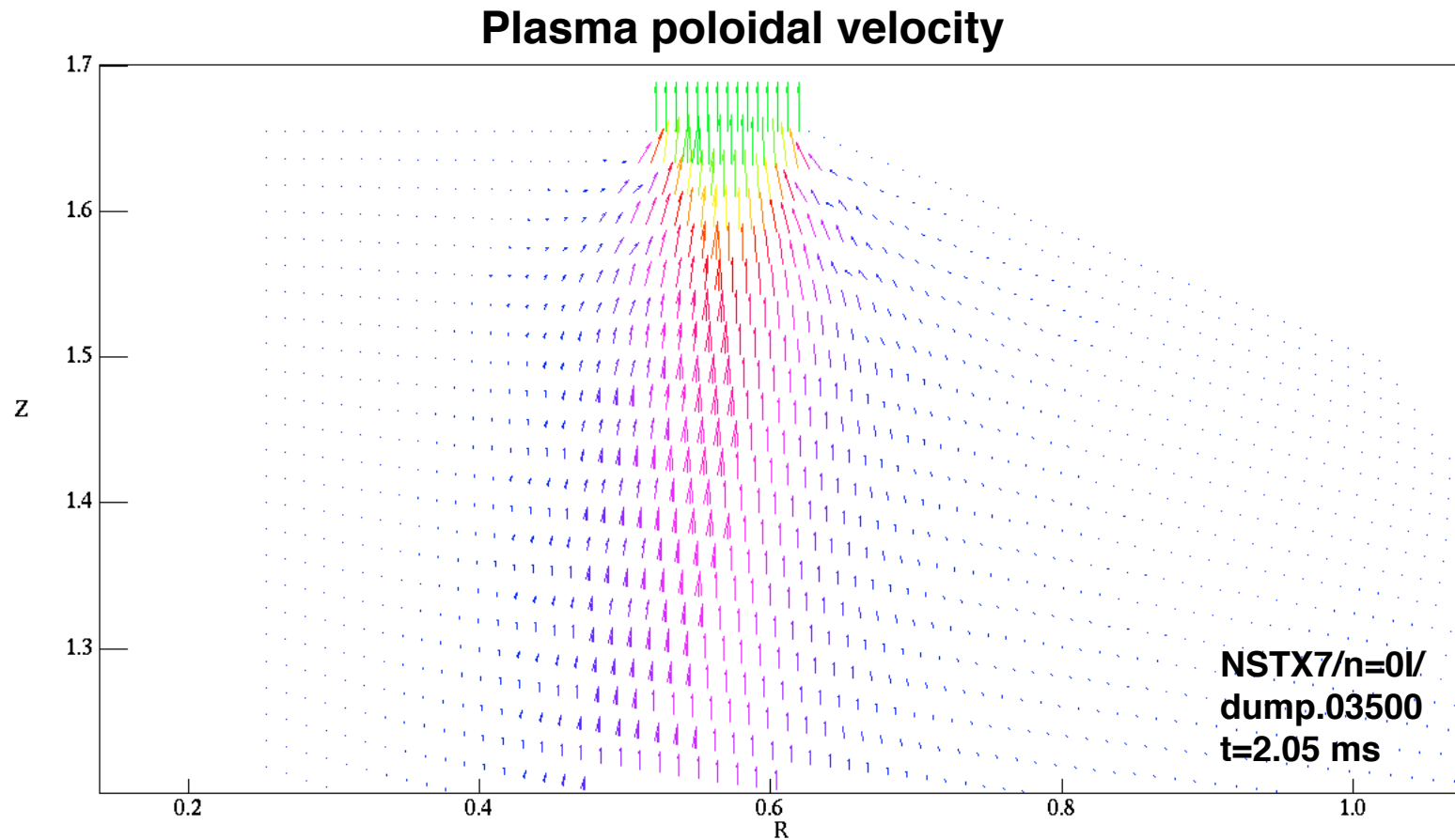
For these simulations:

The toroidal current reaches 50 times the injected current, similar to the experiment

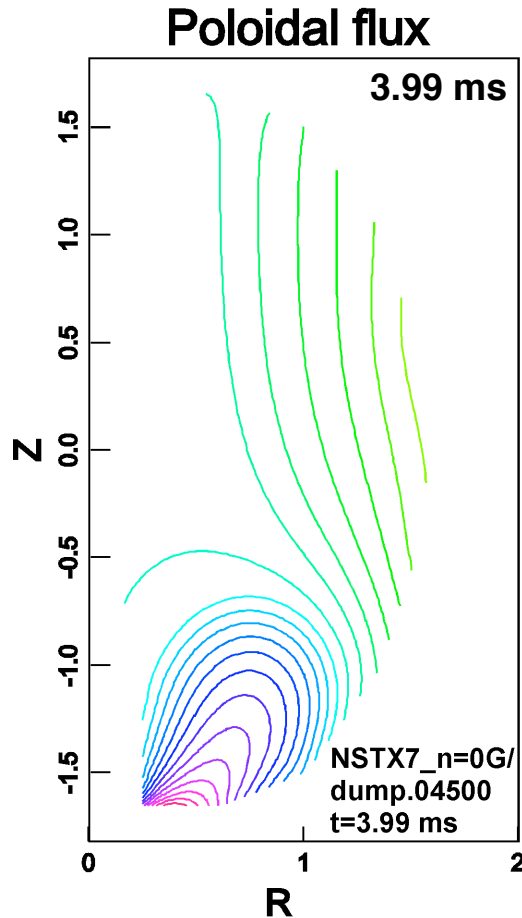
The plasma flow drives the expansion of the flux bubble from the emitter gap



The plasma flow out of the absorber gap sustains a constant vacuum toroidal magnetic flux



Experimental central column calculation: bubble expansion limited — unlike the straight central column



$$E_v = 4 \text{ kV/m}$$
$$rB_\phi = 4 \times 10^{-4} \text{ m-T}$$
$$(I = 8 \text{ kA})$$

Bubble expansion — appears to “hang up” due to currents and flows near the outward-pointing bend in the central column

- This may be due to mesh effects where the boundary bends
- For the straight central column: At low kinetic viscosity, there are also indications of possible mesh effects at bends in the boundary

Calculations with the experimental central column cannot be trusted until this issue is resolved, for example by more careful gridding near the bend

The flux-bubble expansion shows several similarities with spheromak formation

Initial stage of spheromak formation — a bubble forms as plasma is injected from the gun into the simply-connected flux conserver

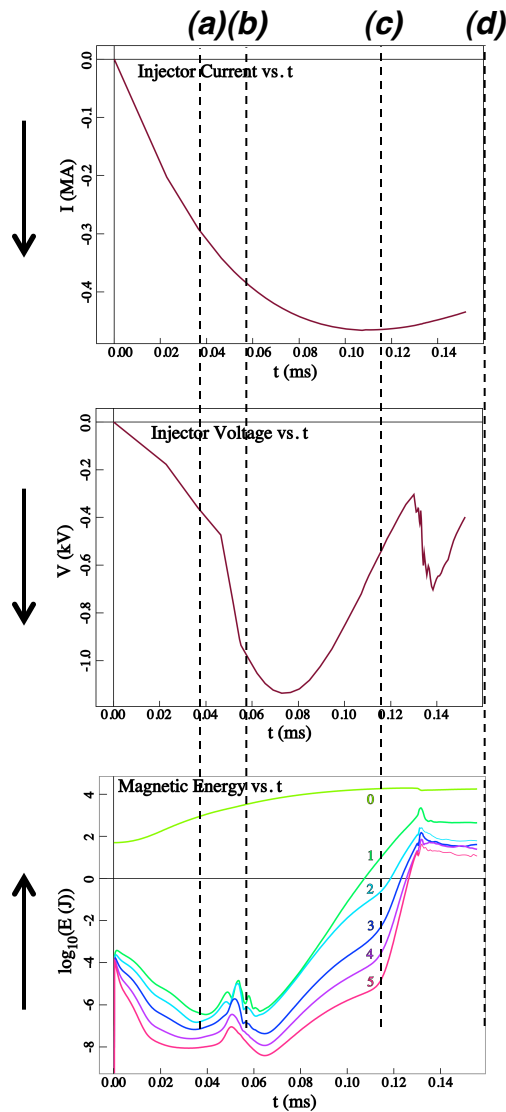
- Toroidal flux is injected — plasma currents flow consistent with the flux

Non-axisymmetric modes grow until a reconnection event occurs

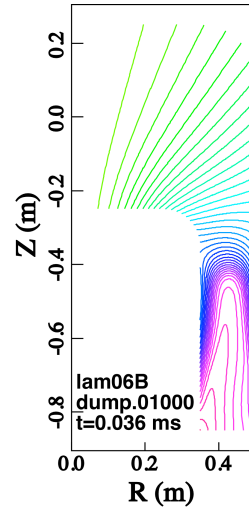
- Toroidal flux — converts into poloidal flux at (approximately) constant helicity. (NSTX simulations to date are axisymmetric and do not change the value of poloidal flux although its distribution is changed (page 9))
- Buildup — continues with reconnection events due to the growth of the non-axisymmetric fields, especially the $n=1$ mode

A quasi-steady, toroidal magnetic geometry is reached
Injected energy and helicity — balanced by losses

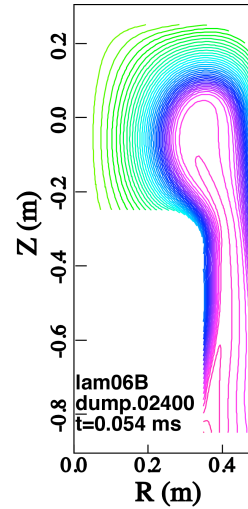
Spheromak MHD simulations: Formation



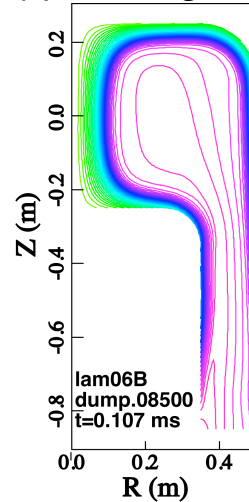
(a) Discharge in gun



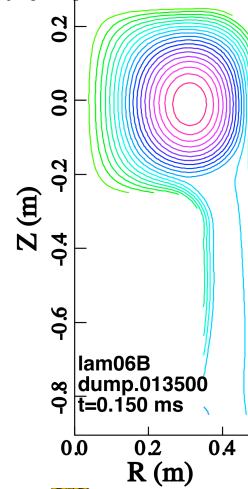
(b) Ejection from gun



(c) Pinching to axis



(d) Spheromak formed



Simulations using the NIMROD code.
Ref.: E. B. Hooper, et al., Phys. Plasmas **15**, 032502 (2008).



Next steps

- (1) Improve the gridding near bends in the boundary — reduce possible mesh effects due to the bends
- (2) Make the applied voltage and current consistent with themselves and the plasma response
 - The current and voltage will be coupled by a power-supply model, as was done for SSPX
- (3) Turn on ohmic heating and the plasma thermal conductivity — determine the temperature self-consistently
- (4) Turn-on the non-axisymmetric modes
- (5) Undertake a detailed comparison with an NSTX experimental shot!